

PAPER • OPEN ACCESS

On the mathematical foundation of full waveform inversion in viscoelastic vertically transverse isotropic media^{*}

To cite this article: Andreas Rieder 2025 *Inverse Problems* **41** 055009

View the [article online](#) for updates and enhancements.

You may also like

- [Full waveform inversion using frequency shift envelope-based global correlation norm for ultrasound computed tomography](#)
Yun Wu, Weicheng Yan, Zhaohui Liu et al.
- [Anthropogenic climate change contribution to wildfire-prone weather conditions in the Cerrado and Arc of deforestation](#)
Sihan Li, Sarah N Sparrow, Friederike E L Otto et al.
- [Physics-guided full waveform inversion using Encoder-Solver convolutional neural networks](#)
Matan M Goren and Eran Treister

On the mathematical foundation of full waveform inversion in viscoelastic vertically transverse isotropic media*

Andreas Rieder 

Department of Mathematics, Karlsruhe Institute of Technology, D-76128 Karlsruhe, Germany

E-mail: andreas.rieder@kit.edu

Received 5 December 2024; revised 31 March 2025

Accepted for publication 23 April 2025

Published 2 May 2025



CrossMark

Abstract

We present a mathematical framework for viscoelastic full waveform inversion (FWI) in vertically transverse isotropic media. FWI can be formulated as the nonlinear inverse problem of identifying parameters in the underlying attenuating anisotropic wave equation given partial wave field measurements (seismograms). From a mathematical point of view, one has to solve an operator equation for the full waveform forward operator, which is the corresponding parameter-to-state map. We give a rigorous definition of this operator, show its Fréchet differentiability, and explicitly characterize the adjoint operator of its Fréchet derivative. Thus, we provide the main ingredients to implement Newton-type/gradient-based regularization schemes for FWI. Our approach can be directly applied to other concepts of anisotropy.

Keywords: full waveform seismic inversion, anisotropic viscoelastic wave equation, adjoint state method, nonlinear inverse and ill-posed problem

* Funded by the Deutsche Forschungsgemeinschaft (DFG, German Research Foundation) - Project-ID 258734477 - SFB 1173.



Original Content from this work may be used under the terms of the [Creative Commons Attribution 4.0 licence](https://creativecommons.org/licenses/by/4.0/). Any further distribution of this work must maintain attribution to the author(s) and the title of the work, journal citation and DOI.

1. Introduction

In seismic imaging we explore the Earth's subsurface. The goal is to determine material parameters, such as the directional variations of velocities of compression and shear waves as well as their attenuations, from partial measurements of wave fields, which have been excited by artificial or natural sources. Here, full waveform inversion (FWI) refers to the corresponding fully nonlinear inverse and ill-posed problem involving the complete parameter-to-state map of the underlying wave propagation model without any further simplifications.

Accurate mathematical models describing the physics of wave propagation are essential to the success of FWI. Since most real rock formations exhibit a directional dependence of wave velocities and attenuation, the resulting anisotropic effects must be taken into account, as has been demonstrated by, e.g. [16, 18, 20]. The most realistic model to date is the viscoelastic wave equation with an anisotropic material law. Several such material laws have been described in the literature modeling various real-world media, see [5] for an overview. As an example, we will limit our analysis to the widely used *vertical transverse isotropy* (VTI) [22], which involves rotational symmetry about the vertical axis and accounts for anisotropy caused by thin horizontal layers.

Since VTI media are characterized by three dimensionless parameters, the Thomsen parameters, FWI in the viscoelastic regime under VTI anisotropy entails the reconstruction of 11 parameter functions, which are in general spatially dependent: bulk density, the vertical velocities of the P- and S-wave, Thomsen parameters, and 5 scaling factors, which specify the attenuation anisotropy. In this work, we rigorously define the corresponding nonlinear operator $\Phi: \mathbf{D}(\Phi) \subset L^\infty(D)^{11} \rightarrow \mathcal{W}$ as the parameter-to-state map of the governing wave equation, where $\mathbf{D}(\Phi)$ is the admissible parameter set and \mathcal{W} is a suitable Hilbert space containing the wave fields. Evaluating $\Phi(\mathbf{m})$ for a given parameter vector \mathbf{m} means solving the wave equation, which we formulate as a first-order hyperbolic system and show to fit the abstract form studied in [15]. Thus, we can explicitly provide the Fréchet derivative $\Phi'(\mathbf{m}) \in \mathcal{L}(L^\infty(D)^{11}, \mathcal{W})$ ¹ and its adjoint operator $\Phi'(\mathbf{m})^* \in \mathcal{L}(\mathcal{W}, (L^\infty(D)^{11})')$, which are the central building blocks for most FWI solvers relying on local linearizations, see, e.g. [4, 8, 17, 24].

The paper is organized as follows. In the next section we discuss the elastic wave equation for VTI media, where we recall the main results of [22] and introduce our notation. Furthermore, we give a sound mathematical formulation of the stiffness tensor, which is the basis for all subsequent considerations. Then we add viscosity to the elastic wave equation in section 3, introducing damping tensors through a slight variation of the generalized standard linear solid rheology due to [25]. Here, we also show that the resulting viscoelastic anisotropic wave equation can be rewritten in an abstract hyperbolic evolution equation as studied in [15]. So we immediately obtain well-posedness and regularity (theorem 3.1). Based on this well-posedness, in section 4 we define the corresponding parameter-to-state map Φ and formulate the inverse problem of FWI, which is locally ill-posed everywhere. Finally, we prove Fréchet differentiability of Φ (theorem 4.2) and express explicitly the adjoint operator of the Fréchet derivative (theorem 4.6). In the last section, we conclude with a brief comment on other anisotropy concepts and the two-dimensional situation.

¹ Throughout $\mathcal{L}(Y, Z)$ denotes the space of bounded linear operators between normed vector spaces Y and Z . Further, $\mathcal{L}(Y) := \mathcal{L}(Y, Y)$.

2. The elastic wave equation for VTI media

Let $D \subset \mathbb{R}^3$ be a Lipschitz domain. Denoting the velocity by $\mathbf{v}: [0, \infty) \times D \rightarrow \mathbb{R}^3$ and the stress by $\boldsymbol{\sigma}: [0, \infty) \times D \rightarrow \mathbb{R}_{\text{sym}}^{3 \times 3}$, the elastic wave equation for VTI media reads

$$\rho \partial_t \mathbf{v} = \operatorname{div} \boldsymbol{\sigma} + \mathbf{f} \quad \text{in } [0, \infty) \times D, \quad (1a)$$

$$\partial_t \boldsymbol{\sigma} = \mathbf{C} \boldsymbol{\varepsilon}(\mathbf{v}) \quad \text{in } [0, \infty) \times D, \quad (1b)$$

where \mathbf{f} denotes the external volume force density and $\rho: D \rightarrow (0, \infty)$ is the mass density. Further,

$$\boldsymbol{\varepsilon}(\mathbf{v}) = \frac{1}{2} \left[(\nabla_x \mathbf{v})^\top + \nabla_x \mathbf{v} \right]$$

is the linearized strain rate.

The linear map $\mathbf{C}: \mathbb{R}_{\text{sym}}^{3 \times 3} \rightarrow \mathbb{R}_{\text{sym}}^{3 \times 3}$ implements Hooke's law and is given in the Voigt notation by

$$\mathbf{C} = \mathbf{T} (c_{3,3}, c_{5,5}, c_{1,1}, c_{6,6}, c_{1,3})^\top \quad (2)$$

where $\mathbf{T} \in \mathcal{L}(\mathbb{R}^5, \mathcal{L}(\mathbb{R}_{\text{sym}}^{3 \times 3}))$ is the tensor-valued map

$$\mathbf{T} (t_{3,3}, t_{5,5}, t_{1,1}, t_{6,6}, t_{1,3})^\top := \begin{pmatrix} t_{1,1} & t_{1,1} - 2t_{6,6} & t_{1,3} & 0 & 0 & 0 \\ t_{1,1} - 2t_{6,6} & t_{1,1} & t_{1,3} & 0 & 0 & 0 \\ t_{1,3} & t_{1,3} & t_{3,3} & 0 & 0 & 0 \\ 0 & 0 & 0 & t_{5,5} & 0 & 0 \\ 0 & 0 & 0 & 0 & t_{5,5} & 0 \\ 0 & 0 & 0 & 0 & 0 & t_{6,6} \end{pmatrix}.$$

The 5 independent real-valued entries of \mathbf{C} are determined to describe layered media that are isotropic in the x_1 - x_2 -plane and anisotropic in all other planes containing the x_3 -direction. These media are called *vertically transverse isotropic* (VTI). In this work, we express the entries of \mathbf{C} by the dimensionless Thomsen parameters ε , δ , and γ , as well as v_p and v_s , which are the P- and S-wave velocities along the x_3 -direction, respectively, see, e.g. [5, chapter 1.2.1]. To model inhomogeneous material, these 5 quantities, like the mass density ρ , are real-valued functions on D , with both velocities attaining only positive values.

The content of the next two paragraphs is basically taken from Thomsen [22]. In VTI media the velocities of plane waves are directional dependent and, for weak anisotropy, are approximated in terms of the Thomsen parameters by

$$\begin{aligned} v_p(\vartheta) &= v_p \left(1 + \delta \sin^2(\vartheta) \cos^2(\vartheta) + \varepsilon \sin^4(\vartheta) \right), \\ v_{SV}(\vartheta) &= v_s \left(1 + \frac{v_p^2}{v_s^2} (\varepsilon - \delta) \sin^2(\vartheta) \cos^2(\vartheta) \right), \\ v_{SH}(\vartheta) &= v_s \left(1 + \gamma \sin^2(\vartheta) \right), \end{aligned}$$

where ϑ is the angle between the x_3 -axis and the direction of wave propagation. The occurrence of shear-wave splitting is the most reliable evidence for the presence of anisotropy.

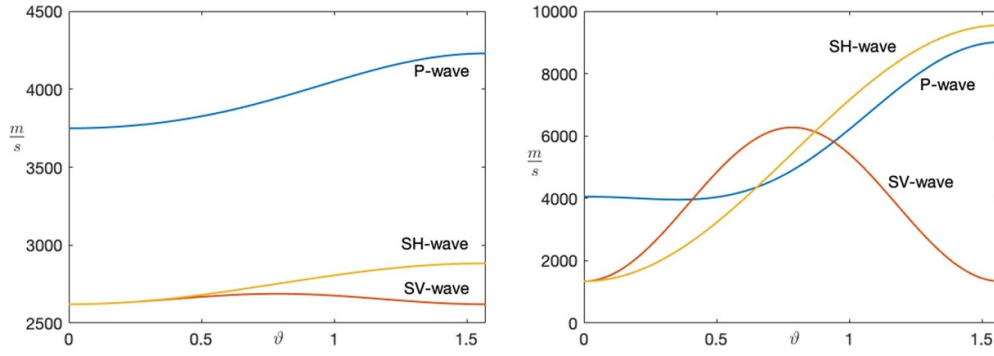


Figure 1. Approximations to P- and S-wave phase velocities for two homogeneous media. The angle $\vartheta \in [0, \pi/2]$ denotes direction of wave propagation relative to the vertical axes. Left: Mesaverde shale at a depth of 3.9 km with $v_p = 3749 \text{ m s}^{-1}$, $v_s = 2621 \text{ m s}^{-1}$, $\varepsilon = 0.128$, $\gamma = 0.1$, and $\delta = 0.078$. Right: biotite crystal with $v_p = 4054 \text{ m s}^{-1}$, $v_s = 1341 \text{ m s}^{-1}$, $\varepsilon = 0.1222$, $\gamma = 6.12$, and $\delta = -0.388$. The numerical values for both materials are taken from [22].

Figure 1 shows the directional variation of P- and S-waves in Mesaverde shale and biotite crystal. The P-wave velocity increases monotonically towards the horizontal direction. The S-wave velocity depends on the polarity: horizontally polarized S-waves (SH) are fastest in the horizontal direction, whereas vertically polarized S-waves (SV) have the maximum velocity at about $\vartheta = \pi/4$. Observe that for the Biotite crystal there are directions of propagation where both S-waves travel faster than the P-wave.

We introduce the P- and S-wave moduli M^2 and μ , which are connected to the P- and S-wave velocities by

$$M = \rho v_p^2 \quad \text{and} \quad \mu = \rho v_s^2. \quad (3)$$

The relations of the Thomsen parameters and the entries of \mathbf{C} are

$$\varepsilon = \frac{c_{1,1} - c_{3,3}}{2c_{3,3}}, \quad \delta = \frac{(c_{1,3} + c_{5,5})^2 - (c_{3,3} - c_{5,5})^2}{2c_{3,3}(c_{3,3} - c_{5,5})}, \quad \gamma = \frac{c_{6,6} - c_{5,5}}{2c_{5,5}}.$$

Additionally,

$$c_{3,3} = M, \quad c_{5,5} = \mu, \quad (4a)$$

yielding

$$\begin{aligned} c_{1,1} &= (2\varepsilon + 1)M, \quad c_{6,6} = (2\gamma + 1)\mu, \\ c_{1,3} &= -\mu \pm \sqrt{(M - \mu)((2\delta + 1)M - \mu)}, \end{aligned} \quad (4b)$$

provided the radicand defining $c_{1,3}$ is non-negative. This is actually a restriction on δ : since $M > \mu$ (see explanation below following (5)) we must have that $2\delta + 1 \geq \mu/M$.

To resolve the ambiguity of which sign to choose in front of the square root in $c_{1,3}$, we consider the case $\delta = 0$ and choose the plus sign: we get $c_{1,3} = M - 2\mu = \lambda$, which is the (first) Lamé coefficient, and this happens to be the physically meaningful case.

² We have that $M = K + 4\mu/3$, where K is the bulk modulus.

The parameters are further subject to the following restrictions which guarantee the positive definiteness of \mathbf{C} as a 6×6 matrix (all principal minors are positive):

$$M > 0, \quad \mu > 0, \quad 2\varepsilon + 1 > 0, \quad 2\gamma + 1 > 0, \quad 2\delta + 1 \geq \frac{\mu}{M}, \quad \frac{M}{\mu} > \frac{2\gamma + 1}{2\varepsilon + 1}, \quad (5a)$$

$$((2\varepsilon + 1)M - (2\gamma + 1)\mu)M > \left(\sqrt{(M - \mu)((2\delta + 1)M - \mu)} - \mu \right)^2. \quad (5b)$$

Observe that $(2\varepsilon + 1)M - (2\gamma + 1)\mu > 0$ by the lower bound on M/μ . Setting $\varepsilon = \delta = \gamma = 0$ in (5b) yields $3M > 4\mu$ (or $3v_p^2 > 4v_s^2$, in particular $v_p > v_s$) which indicates that compression waves travel significantly faster than shear waves in isotropic media.

Remark 2.1. In this remark we comment further on the physical aspects of the conditions in (5). As already mentioned above, they originate from the positive definiteness of the Hooke tensor \mathbf{C} . This property of \mathbf{C} is a physical requirement so that the strain-energy volume density $\frac{1}{2} \sum_{i,j} (\mathbf{C}\varepsilon(\mathbf{u}))_{ij} \varepsilon(\mathbf{u})_{ij}$ attains its minimum at zero strain state ($\mathbf{u} = 0$) and always increases when the medium is deformed. As far as the author knows, the resulting condition $v_p > \sqrt{4/3} v_s$ is satisfied for real material³. Therefore, we can conclude by continuity that (5) holds for natural materials and small absolute values of the Thomsen parameters. Most of the measured parameters listed in [22] have rather small absolute magnitudes (in relation to M/μ), so it seems that they satisfy (5) (samples taken have confirmed this conjecture, for example both sets of values reported in the caption of figure 1). A full physical interpretation of the parameters is beyond the scope of the present work. In a nutshell, they have the following meaning: ε describes the level of P-wave anisotropy, γ the level of SH-wave anisotropy, and δ the level of P-wave moveout anisotropy; for all details we refer to the section ‘Weak Anisotropy’ of [22, page 1957 ff] and to [23, section 1.2.2].

Finally, the inequalities in (5) are invariant under the same positive scaling of M and m . This was to be expected since the validity of (5) should be independent of the physical units in which the P- and S-wave moduli are expressed. Consequently, we may replace M and μ by v_p^2 and v_s^2 , respectively.

2.1. Stiffness tensor as a function of the parameters

From here on, we treat the stiffness matrix (2) as a mapping taking 5 real values as arguments:

$$\mathbf{C}: \mathbf{D}(\mathbf{C}) \subset \mathbb{R}^5 \rightarrow \mathcal{L}(\mathbb{R}_{\text{sym}}^{3 \times 3}), \quad \mathbf{q} = (q_1, q_2, q_3, q_4, q_5)^\top \mapsto \mathbf{C}(\mathbf{q}),$$

where the entries of $\mathbf{C}(\mathbf{q})$ are set in agreement with (3) and (4) (with the plus sign in front of the root in $c_{1,3}$):

$$c_{1,1}(\mathbf{q}) = (2q_3 + 1)q_1, \quad c_{3,3}(\mathbf{q}) = q_1, \quad c_{5,5}(\mathbf{q}) = q_2, \quad c_{6,6}(\mathbf{q}) = (2q_4 + 1)q_2, \quad (6a)$$

$$c_{1,3}(\mathbf{q}) = q_2 + \sqrt{(q_1 - q_2)((2q_5 + 1)q_1 - q_2)}. \quad (6b)$$

³ If Poisson’s ratio of the homogeneous material is in $[0, 0.5)$ then $v_p \geq \sqrt{2}v_s > \sqrt{4/3}v_s$, see, e.g. [11, (9.30)]. This is the case for many minerals and rock types, see, e.g. [10, table 3 and figure 4].

Thus, $\mathbf{C}(\mathbf{q}) = \mathbf{T}(c_{3,3}(\mathbf{q}), c_{5,5}(\mathbf{q}), c_{1,1}(\mathbf{q}), c_{6,6}(\mathbf{q}), c_{1,3}(\mathbf{q}))^\top$.

We will define the domain of definition $\mathbf{D}(\mathbf{C})$ of \mathbf{C} so that it includes material parameters $(M, \mu, \varepsilon, \gamma, \delta)$ which satisfy (5). Moreover, $\mathbf{D}(\mathbf{C})$ will be compact with an open interior. To this end, choose $\underline{q}_i, \bar{q}_i \in \mathbb{R}$ with $\underline{q}_i < \bar{q}_i$ for $i = 1, \dots, 5$, where $0 < \underline{q}_i$, $i = 1, 2$, and $-1/2 < \underline{q}_i$, $0 < \bar{q}_i$, $i = 3, 4, 5$. Now, with $r > 0$ define

$$\mathbf{D}(\mathbf{C}) := \left\{ \mathbf{q} \in \bigtimes_{i=1}^5 [\underline{q}_i, \bar{q}_i] : \frac{q_1}{q_2} \geq r + \max \left\{ \frac{2q_4 + 1}{2q_3 + 1}, \frac{1}{2q_5 + 1} \right\}, \right. \\ \left. ((2q_3 + 1)q_1 - (2q_4 + 1)q_2)q_1 \geq r + \left(\sqrt{(q_1 - q_2)((2q_5 + 1)q_1 - q_2)} - q_2 \right)^2 \right\}.$$

Obviously, $\mathbf{D}(\mathbf{C})$ is compact and we can assume a non-empty interior: for instance, in case of $3\underline{q}_1 > 4\bar{q}_2$ we fix an $r > 0$ such that $r \leq \max\{(3\underline{q}_1 - 4\bar{q}_2)\underline{q}_2, \underline{q}_1/\bar{q}_2 - 1\}$. Then, $\mathcal{Q} = (\underline{q}_1, \bar{q}_1) \times (\underline{q}_2, \bar{q}_2) \times \{0\} \times \{0\} \times \{0\} \subset \mathbf{D}(\mathbf{C})$. Moreover, by continuity, for each element in \mathcal{Q} there exists a neighborhood which is contained in $\mathbf{D}(\mathbf{C})$. Note that the limiting values $\underline{q}_i, \bar{q}_i$ can be adjusted so that $\mathbf{D}(\mathbf{C})$ includes the relevant material parameters for a certain physical setting, see, e.g. table 1 in [22] for measured anisotropy values in sedimentary rocks.

One immediate and important consequence of the properties of $\mathbf{D}(\mathbf{C})$ is the uniform positive definiteness of $\mathbf{C}(\mathbf{q})$ for $\mathbf{q} \in \mathbf{D}(\mathbf{C})$ (as a 6×6 matrix): there are constants $0 < c \leq C$ such that

$$c|w|^2 \leq w^\top \mathbf{C}(\mathbf{q})w \leq C|w|^2 \quad \text{for any } w \in \mathbb{R}^6 \text{ uniformly in } \mathbf{q} \in \mathbf{D}(\mathbf{C}). \quad (7)$$

Observe that c tends to zero as $r \searrow 0$.

Further, \mathbf{C} is Fréchet differentiable at any $\mathbf{q} \in \text{int}(\mathbf{D}(\mathbf{C}))$. In fact, for $\mathbf{h} \in \mathbb{R}^5$, $\mathbf{C}'(\mathbf{q})\mathbf{h} \in \mathcal{L}(\mathbb{R}_{\text{sym}}^{3 \times 3})$ is represented by

$$\mathbf{C}'(\mathbf{q})\mathbf{h} = \begin{pmatrix} c'_{1,1}(\mathbf{q})\mathbf{h} & (c'_{1,1} - 2c'_{6,6})(\mathbf{q})\mathbf{h} & c'_{1,3}(\mathbf{q})\mathbf{h} & 0 & 0 & 0 \\ (c'_{1,1} - 2c'_{6,6})(\mathbf{q})\mathbf{h} & c'_{1,1}(\mathbf{q})\mathbf{h} & c'_{1,3}(\mathbf{q})\mathbf{h} & 0 & 0 & 0 \\ c'_{1,3}(\mathbf{q})\mathbf{h} & c'_{1,3}(\mathbf{q})\mathbf{h} & h_1 & 0 & 0 & 0 \\ 0 & 0 & 0 & h_2 & 0 & 0 \\ 0 & 0 & 0 & 0 & h_2 & 0 \\ 0 & 0 & 0 & 0 & 0 & c'_{6,6}(\mathbf{q})\mathbf{h} \end{pmatrix} \\ = \mathbf{T}(h_1, h_2, c'_{1,1}(\mathbf{q})\mathbf{h}, c'_{6,6}(\mathbf{q})\mathbf{h}, c'_{1,3}(\mathbf{q})\mathbf{h})^\top \quad (8a)$$

with

$$c'_{1,1}(\mathbf{q})\mathbf{h} = (2q_3 + 1)h_1 + 2q_1h_3, \quad c'_{6,6}(\mathbf{q})\mathbf{h} = (2q_4 + 1)h_2 + 2q_2h_4, \quad (8b)$$

$$c'_{1,3}(\mathbf{q})\mathbf{h} = \frac{(q_1(2q_2 + 1) - q_2(q_5 + 1))h_1 + (q_2 - q_1(q_5 + 1))h_2 + q_1(q_1 - q_2)h_5}{\sqrt{(q_1 - q_2)((2q_5 + 1)q_1 - q_2)}} - h_2. \quad (8c)$$

For $\mathbf{q} \in \mathbf{D}(\mathbf{C})$ the inverse matrix

$$\tilde{\mathbf{C}}(\mathbf{q}) := \mathbf{C}(\mathbf{q})^{-1} \quad (9)$$

exists and is Fréchet differentiable in the interior of $\mathbf{D}(\mathbf{C})$ according to

$$\tilde{\mathbf{C}}'(\mathbf{q})\mathbf{h} = -\tilde{\mathbf{C}}(\mathbf{q})\mathbf{C}'(\mathbf{q})\mathbf{h}\tilde{\mathbf{C}}(\mathbf{q}) \quad (10)$$

for which we have applied the chain rule and the derivative of matrix inversion, see, e.g. [6, example 16.14].

3. Adding viscosity to VTI media

In contrast to elastic materials, viscoelastic materials possess a memory effect, whereby the stress state at a given instant is subject to the cumulative deformation history of the material [7].

Instead of (1b) we allow a retarded material law

$$\partial_t \boldsymbol{\sigma}(t, x) = \mathbf{C}(0) \boldsymbol{\varepsilon}(\mathbf{v}(t, x)) + \int_0^t \partial_s \mathbf{C}(t-s) \boldsymbol{\varepsilon}(\mathbf{v}(s, x)) \, ds, \quad (t, x) \in [0, \infty) \times D,$$

where $\mathbf{C}: [0, \infty) \rightarrow \mathcal{L}(\mathbb{R}_{\text{sym}}^{3 \times 3})$ is the time-dependent Hooke tensor.

In the *generalized standard linear solid* rheology, see, e.g. [1, 9, 19, 21], one defines

$$\mathbf{C}(t) := \mathbf{C}(\mathbf{p}) + \sum_{l=1}^L \exp\left(-\frac{t}{t_{\sigma,l}}\right) \mathbf{C}_u(\mathbf{p}, \boldsymbol{\tau})$$

with relaxation times $t_{\sigma,l} > 0$, $l = 1, \dots, L \in \mathbb{N}$, where $\mathbf{p} = (M, \mu, \varepsilon, \gamma, \delta)^\top$ contains the material parameters and $\boldsymbol{\tau} := (\tau_p, \tau_s, \tau_e, \tau_g, \tau_d)^\top$ collects the positive scaling factors of the respective material parameters. The entries of the tensor $\mathbf{C}_u(\mathbf{p}, \boldsymbol{\tau}) \in \mathcal{L}(\mathbb{R}_{\text{sym}}^{3 \times 3})$ are the unrelaxed moduli, that is,

$$\mathbf{C}_u(\mathbf{q}, \boldsymbol{\tau}) := \mathbf{T}(\boldsymbol{\tau} \odot \mathbf{c}(\mathbf{q})), \quad \mathbf{c}(\mathbf{q}) := (c_{3,3}, c_{5,5}, c_{1,1}, c_{6,6}, c_{1,3})^\top, \quad \mathbf{q} \in \mathbf{D}(\mathbf{C}), \quad (11)$$

where the $c_{i,j}$'s are functions of \mathbf{q} via (6) and the binary operator symbol \odot denotes component-wise multiplication.

Following the presentation in [4] and [6, chapter 1.5], which is based on [25], we introduce $L \in \mathbb{N}$ damping tensors $\boldsymbol{\sigma}_l: [0, \infty) \times D \rightarrow \mathbb{R}_{\text{sym}}^{3 \times 3}$,

$$\boldsymbol{\sigma}_l(t) := \boldsymbol{\sigma}_{l,0} + \int_0^t \exp\left(-\frac{s-t}{t_{\sigma,l}}\right) \mathbf{C}_u(\mathbf{p}, \boldsymbol{\tau}) \boldsymbol{\varepsilon}(\mathbf{v}(s)) \, ds, \quad l = 1, \dots, L,$$

and the corresponding stress decomposition $\boldsymbol{\sigma} = \boldsymbol{\sigma}_0 + \sum_{l=1}^L \boldsymbol{\sigma}_l$. This decomposition yields the first order system for viscoelastic waves in VTI media

$$\varrho \partial_t \mathbf{v} = \operatorname{div} \left(\sum_{l=0}^L \boldsymbol{\sigma}_l \right) + \mathbf{f} \quad \text{in } [0, \infty) \times D, \quad (12a)$$

$$\partial_t \boldsymbol{\sigma}_0 = \mathbf{C}(\mathbf{p}) \boldsymbol{\varepsilon}(\mathbf{v}) \quad \text{in } [0, \infty) \times D, \quad (12b)$$

$$t_{\sigma,l} \partial_t \boldsymbol{\sigma}_l = t_{\sigma,l} \mathbf{C}_u(\mathbf{p}, \boldsymbol{\tau}) \boldsymbol{\varepsilon}(\mathbf{v}) - \boldsymbol{\sigma}_l, \quad l = 1, \dots, L, \quad \text{in } [0, \infty) \times D, \quad (12c)$$

with initial conditions

$$\mathbf{v}(0) = \mathbf{v}_0 \quad \text{and} \quad \boldsymbol{\sigma}_l(0) = \boldsymbol{\sigma}_{l,0}, \quad l = 0, \dots, L. \quad (12d)$$

By continuity, we can find bounds $0 < \underline{\tau}_i \leq 1 < \bar{\tau}_i$, $i = 1, \dots, 5$, such that

$\mathbf{C}_u(\mathbf{p}, \boldsymbol{\tau})$ is positive definite and satisfies (7) with adjusted constants

$$\text{for any } \boldsymbol{\tau}(\cdot) \in \bigtimes_{i=1}^5 [\underline{\tau}_i, \bar{\tau}_i] \text{ and any } \mathbf{p}(\cdot) \in \mathbf{D}(\mathbf{C}) \text{ a.e. in } D. \quad (13a)$$

Further, we require bounds for the bulk density:

$$0 < \rho_{\min} \leq \rho(\cdot) \leq \rho_{\max} < \infty \text{ a.e. in } D. \quad (13b)$$

Under these assumptions, the existence and uniqueness theory for abstract evolution equations developed in [14, 15] can be applied to (12) when expressed as

$$Bu'(t) + (A + BQ)u(t) = f(t), \quad t \in [0, \infty), \quad u(0) = u_0, \quad (14)$$

where

$$u(t) = (\mathbf{v}(t, \cdot), \boldsymbol{\sigma}_0(t, \cdot), \dots, \boldsymbol{\sigma}_L(t, \cdot))^\top, \quad f(t) = (\mathbf{f}(t, \cdot), \mathbf{0}, \dots, \mathbf{0})^\top, \\ \text{and } u_0 = (\mathbf{v}_0, \boldsymbol{\sigma}_{0,0}, \dots, \boldsymbol{\sigma}_{L,0})^\top.$$

The operators A , B , and Q are defined on the Hilbert space

$$X := L^2(D, \mathbb{R}^3) \times L^2(D, \mathbb{R}_{\text{sym}}^{3 \times 3})^{1+L},$$

which carries the inner product

$$\left\langle (\mathbf{v}, \boldsymbol{\sigma}_0, \dots, \boldsymbol{\sigma}_L)^\top, (\mathbf{w}, \boldsymbol{\psi}_0, \dots, \boldsymbol{\psi}_L)^\top \right\rangle_X := \int_D \left(\mathbf{v} \cdot \mathbf{w} + \sum_{l=0}^L \boldsymbol{\sigma}_l : \boldsymbol{\psi}_l \right) dx$$

with the colon denoting the Frobenius inner product on $\mathbb{R}^{3 \times 3}$.

For $w = (\mathbf{w}, \boldsymbol{\psi}_0, \dots, \boldsymbol{\psi}_L)^\top \in X$ we define, recalling (9),

$$Bw := \begin{pmatrix} \varrho \mathbf{w} \\ \tilde{\mathbf{C}}(\mathbf{p}) \boldsymbol{\psi}_0 \\ \tilde{\mathbf{C}}_u(\mathbf{p}, \boldsymbol{\tau}) \boldsymbol{\psi}_1 \\ \vdots \\ \tilde{\mathbf{C}}_u(\mathbf{p}, \boldsymbol{\tau}) \boldsymbol{\psi}_L \end{pmatrix} \quad \text{and} \quad Qw := \begin{pmatrix} \mathbf{0} \\ \mathbf{0} \\ \frac{1}{t_{\sigma,1}} \boldsymbol{\psi}_1 \\ \vdots \\ \frac{1}{t_{\sigma,L}} \boldsymbol{\psi}_L \end{pmatrix}. \quad (15)$$

In view of (7), the collection of self-adjoint operators

$$\{B = B(\rho, \mathbf{p}, \boldsymbol{\tau}) : \rho, \mathbf{p}, \boldsymbol{\tau} \text{ satisfy (13)}\} \subset \mathcal{L}(X) \quad (16)$$

is uniformly positive definite and uniformly bounded.

Finally, the differential operator

$$Aw := - \begin{pmatrix} \operatorname{div} \left(\sum_{l=0}^L \boldsymbol{\psi}_l \right) \\ \boldsymbol{\varepsilon}(\mathbf{w}) \\ \vdots \\ \boldsymbol{\varepsilon}(\mathbf{w}) \end{pmatrix} \quad (17a)$$

is defined on⁴

$$\mathbf{D}(A) := H_0^1(D, \mathbb{R}^3) \times \{ \boldsymbol{\sigma} \in L^2(D, \mathbb{R}_{\text{sym}}^{3 \times 3}) : \operatorname{div} \boldsymbol{\sigma}_{*,j} \in L^2(D), j = 1, 2, 3 \}^{1+L}. \quad (17b)$$

⁴ In our definition of $\mathbf{D}(A)$, we impose zero Dirichlet boundary conditions for the velocity on all of $\operatorname{bd}(D)$. However, we could also split the boundary into a part where we have a Dirichlet condition for the velocity and a part where a Neumann condition applies to the stress, see [15, section 4].

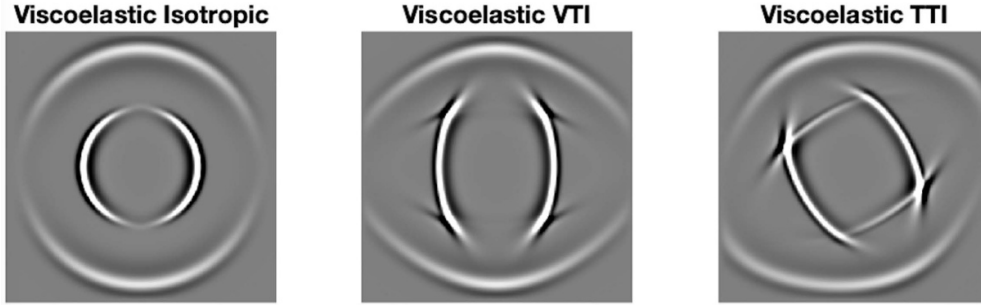


Figure 2. Numerical simulations of the vertical component of the particle velocity excited by a vertical point force in the middle. The snapshots show P- and SV-waves and the effects of attenuation for VTI and tilted transverse isotropic anisotropy (TTI), which is a rotated version of VTI, see section 5.1. The homogeneous anisotropic VTI model is that of Greenhorn shale [13]. In the TTI model the symmetry axis has been rotated counter-clockwise by the angle $\theta_v = \pi/6$. Attenuation is assumed to be isotropic with $\tau_p = \tau_s = 0.25$ and $L = 1$. The simulations were kindly provided by Thomas Bohlen (Geophysical Institute, KIT) and computed with the FDTD⁵ code SOFI2D, which is available from <https://gitlab.kit.edu/kit/gpi/ag/software/sofi2d>.

Within this setting, $A: D(A) \subset X \rightarrow X$ is a maximal monotone operator [15, lemma 4.1].

Now, all assumptions of the abstract framework from [15, section 3] are met and we can conclude the following well-posedness results for the viscoelastic wave equation in VTI media.

Theorem 3.1. *Assume that $p(\cdot) \in D(C)$ a.e. in D . Let (7) and (13) hold.*

If $(v_0, \sigma_{0,0}, \dots, \sigma_{L,0})^\top \in D(A)$ and $f \in W^{1,1}([0, \infty), L^2(D, \mathbb{R}^3))$, then (12) admits a unique classical solution $(v, \sigma_0, \dots, \sigma_L)^\top \in C([0, \infty), D(A)) \cap C^1([0, \infty), X)$.

Under less regularity, $(v_0, \sigma_{0,0}, \dots, \sigma_{L,0})^\top \in X$ and $f \in L^1_{\text{loc}}([0, \infty), L^2(D, \mathbb{R}^3))$, (12) admits a unique mild/weak solution $(v, \sigma_0, \dots, \sigma_L)^\top \in C([0, \infty), X)$ (see, e.g. [12] for the definition of mild/weak solutions).

Figure 2 illustrates the effects of damped wave propagation under different anisotropies in two spatial dimensions; see section 5.2 for the two-dimensional situation.

The frequency dependence of wave propagation in real media about a center frequency ω_0 is modeled via a constant quality factor Q , which is the ratio of the full energy to the dissipated energy, see [1]. In this way the relaxations times $t_{\sigma,l} = t_{\sigma,l}(\omega_0) > 0$ are determined by a least squares method [2, 3]. The frequency-dependent P- and S-wave moduli are now given by

$$M = \frac{\rho v_p^2}{1 + \tau_p \alpha} \quad \text{and} \quad \mu = \frac{\rho v_s^2}{1 + \tau_s \alpha} \quad \text{with} \quad \alpha := \sum_{l=1}^L \frac{\omega_0^2 t_{\sigma,l}^2}{1 + \omega_0^2 t_{\sigma,l}^2}, \quad (18)$$

replacing (3).

4. The inverse problem

FWI in VTI media under the viscoelastic regime entails the reconstruction of the 11 parameter functions $\rho, \pi = (v_p, v_s, \varepsilon, \gamma, \delta)^\top$, and $\tau = (\tau_p, \tau_s, \tau_e, \tau_g, \tau_d)^\top$ from (partial) wave field measurements.

⁵ FDTD: finite difference time domain.

4.1. The setting

To formulate this seismic inverse problem we need to define the full waveform forward operator Φ . In a first step we introduce the auxiliary operator $\tilde{\Phi}$ with domain⁶

$$\mathbf{D}(\tilde{\Phi}) := \left\{ (\rho, \mathbf{p}, \boldsymbol{\tau})^\top \in L^\infty(D)^{11} : (\rho, \mathbf{p}, \boldsymbol{\tau})^\top \text{ satisfy (13)} \right\}$$

according to

$$\tilde{\Phi} : \mathbf{D}(\tilde{\Phi}) \subset L^\infty(D)^{11} \rightarrow L^2([0, T], X), \quad (\rho, \mathbf{p}, \boldsymbol{\tau})^\top \mapsto (\mathbf{v}, \boldsymbol{\sigma}_0, \dots, \boldsymbol{\sigma}_L)^\top|_{[0, T]},$$

where $T > 0$ is the observation period and $(\mathbf{v}, \boldsymbol{\sigma}_0, \dots, \boldsymbol{\sigma}_L)^\top$ is the unique classical solution of (12) for a given $\mathbf{f} \in W^{1,1}([0, \infty), L^2(D, \mathbb{R}^3))$ and initial values $(\mathbf{v}_0, \boldsymbol{\sigma}_{0,0}, \dots, \boldsymbol{\sigma}_{L,0})^\top \in \mathbf{D}(A)$. This mapping is well defined, see theorem 3.1.

The final ingredient for Φ is the parameter transformation

$$\begin{aligned} P : \mathbf{D}(P) \subset L^\infty(D)^{11} &\rightarrow L^\infty(D)^{11}, \\ (p_0, p_1, p_2, \dots, p_{10})^\top &\mapsto \left(p_0, \frac{p_0 p_1^2}{1 + \alpha p_6}, \frac{p_0 p_2^2}{1 + \alpha p_7}, p_3, \dots, p_{10} \right)^\top, \end{aligned}$$

where $\mathbf{D}(P) = L^\infty(D)^6 \times \mathcal{T}$ with

$$\mathcal{T} := \left\{ \mathbf{w} \in L^\infty(D)^5 : \mathbf{w}(\cdot) \in \bigtimes_{i=1}^5 [\underline{\tau}_i, \bar{\tau}_i] \text{ a.e. in } D \right\}.$$

Note that P implements the change of parameters due to (18):

$$P(\rho, v_p, v_s, \varepsilon, \gamma, \delta, \tau_p, \tau_s, \tau_e, \tau_g, \tau_d) = (\rho, \mathbf{M}, \mu, \varepsilon, \gamma, \delta, \tau_p, \tau_s, \tau_e, \tau_g, \tau_d)^\top,$$

in short, $P(\rho, \boldsymbol{\pi}, \boldsymbol{\tau}) = (\rho, \mathbf{p}, \boldsymbol{\tau})^\top$.

Remark 4.1. A change in model parameters can be accounted for by adjusting the transformation P .

Now, we define the full waveform forward operator $\Phi := \tilde{\Phi} \circ P$ on $\mathbf{D}(\Phi) := P^{-1}(\mathbf{D}(\tilde{\Phi}))$, the preimage of $\mathbf{D}(\tilde{\Phi})$ under P , by

$$\Phi : \mathbf{D}(\Phi) \subset L^\infty(D)^{11} \rightarrow L^2([0, T], X), \quad (\rho, \boldsymbol{\pi}, \boldsymbol{\tau})^\top \mapsto \tilde{\Phi}(P(\rho, \boldsymbol{\pi}, \boldsymbol{\tau})). \quad (19)$$

Since P is continuous, we can ensure, by appropriate choices of ρ_{\min}, ρ_{\max} , and the limiting values appearing in the definitions of $\mathbf{D}(C)$ and \mathcal{T} , that $\mathbf{D}(\Phi)$ has a non-empty interior, which contains all 11 physically relevant parameters $(\rho, \boldsymbol{\pi}, \boldsymbol{\tau})^\top$. A more explicit expression for $\mathbf{D}(\Phi)$ is not needed in what follows. It is hard to find anyway and would not gain us any deeper insight.

For the complete formulation of the inverse problem we model the measurement process by the linear seismogram operator $S : L^2([0, T], X) \rightarrow \mathbb{R}^N$, which samples certain components of at finitely many times in $[0, T]$ and receiver positions in D (or at its boundary). Here, N is the number of sample points (time points \times number of receivers). Recall that $\sum_{l=0}^L \boldsymbol{\sigma}_l$ adds up to the stress $\boldsymbol{\sigma}$, some components of which can actually be observed, unlike the individual

⁶ For simplicity, here and later we use $(\rho, \mathbf{p}, \boldsymbol{\tau})^\top$ instead of the correct expression $(\rho, \mathbf{p}^\top, \boldsymbol{\tau}^\top)^\top$. Further, we will write $\tilde{\Phi}(\rho, \mathbf{p}, \boldsymbol{\tau})$ for $\tilde{\Phi}((\rho, \mathbf{p}, \boldsymbol{\tau})^\top)$ (likewise for other mappings).

σ_l 's which have no physical meaning. The images of S are called seismograms. Now, FWI in VTI media under the viscoelastic regime consists of solving the nonlinear equation

$$S\Phi(\rho, \pi, \tau) = s \quad (20)$$

for a given seismogram $s \in \mathbb{R}^N$.

The inverse problem (20) is locally ill-posed at any parameter point $\mathbf{m}^+ \in \text{int}(\mathbf{D}(\Phi))$ in the following sense: in any neighborhood of \mathbf{m}^+ there exists a sequence $\{\mathbf{m}_k\}$ with

$$\lim_{k \rightarrow \infty} \|\Phi(\mathbf{m}_k) - \Phi(\mathbf{m}^+)\|_{L^2([0,T],X)} = 0 \quad \text{but } \mathbf{m}_k \not\rightarrow \mathbf{m}^+ \text{ in } L^\infty(D)^{11}. \quad (21)$$

The validity of (21) can be shown by reproducing the proof of theorem 4.3 in [15].

4.2. Differentiability and adjoint

The adequate solution of the ill-posed seismic inverse problem (20) requires regularization, typically by iterative schemes based on local linearization. Required ingredients are Fréchet differentiability and the adjoint operator of the Fréchet derivative. We provide both for the full waveform forward operator Φ , where we will rely on the results from [15] for the abstract evolution equation (14).

4.2.1. The derivate. We start by giving the Fréchet derivative of P . For $(\rho, \pi, \tau)^\top \in \mathbf{D}(P)$ and $(\hat{\rho}, \hat{\pi}, \hat{\tau})^\top \in L^\infty(D)^{11}$ we have

$$P'(\rho, \pi, \tau) \begin{bmatrix} \hat{\rho} \\ \hat{\pi} \\ \hat{\tau} \end{bmatrix} = \left(\hat{\rho}, \frac{v_p^2}{1 + \alpha\tau_p} \hat{\rho} + \frac{2\rho v_p}{1 + \alpha\tau_p} \hat{v}_p - \frac{\rho v_p^2 \alpha}{(1 + \alpha\tau_p)^2} \hat{\tau}_p, \frac{v_s^2}{1 + \alpha\tau_s} \hat{\rho} + \frac{2\rho v_s}{1 + \alpha\tau_s} \hat{v}_s - \frac{\rho v_s^2 \alpha}{(1 + \alpha\tau_s)^2} \hat{\tau}_s, \hat{\varepsilon}, \hat{\gamma}, \hat{\delta}, \hat{\tau}_p, \hat{\tau}_s, \hat{\tau}_e, \hat{\tau}_g, \hat{\tau}_d \right)^\top \in L^\infty(D)^{11}.$$

Further, we differentiate $B: \mathbf{D}(\Phi) \subset L^\infty(D)^{11} \rightarrow \mathcal{L}(X)$, as defined in (15) and (16), to get

$$B'(\rho, \mathbf{p}, \tau) \begin{bmatrix} \hat{\rho} \\ \hat{\mathbf{p}} \\ \hat{\tau} \end{bmatrix} \begin{pmatrix} \mathbf{w} \\ \psi_0 \\ \vdots \\ \psi_L \end{pmatrix} = \begin{pmatrix} \hat{\rho} \mathbf{w} \\ \tilde{\mathbf{C}}'(\mathbf{p}) \hat{\mathbf{p}} \psi_0 \\ \tilde{\mathbf{C}}'_u(\mathbf{p}, \tau) \begin{bmatrix} \hat{\mathbf{p}} \\ \hat{\tau} \end{bmatrix} \psi_1 \\ \vdots \\ \tilde{\mathbf{C}}'_u(\mathbf{p}, \tau) \begin{bmatrix} \hat{\mathbf{p}} \\ \hat{\tau} \end{bmatrix} \psi_L \end{pmatrix} \in X$$

for $(\mathbf{w}, \psi_0, \dots, \psi_L)^\top \in X$ where, by analogy to (10),

$$\tilde{\mathbf{C}}'_u(\mathbf{p}, \tau) \begin{bmatrix} \hat{\mathbf{p}} \\ \hat{\tau} \end{bmatrix} = -\tilde{\mathbf{C}}_u(\mathbf{p}, \tau) \mathbf{C}'_u(\mathbf{p}, \tau) \begin{bmatrix} \hat{\mathbf{p}} \\ \hat{\tau} \end{bmatrix} \tilde{\mathbf{C}}_u(\mathbf{p}, \tau). \quad (22)$$

In view of (11) we get by the chain rule and the linearity of \mathbf{T} that

$$\mathbf{C}'_u(\mathbf{p}, \tau) \begin{bmatrix} \hat{\mathbf{p}} \\ \hat{\tau} \end{bmatrix} = \mathbf{T}(\hat{\tau} \odot \mathbf{c}(\mathbf{p}) + \tau \odot \mathbf{c}'(\mathbf{p}) \hat{\mathbf{p}}) = \mathbf{C}_u(\mathbf{p}, \hat{\tau}) + \mathbf{T}(\tau \odot \mathbf{c}'(\mathbf{p}) \hat{\mathbf{p}}) \quad (23a)$$

with, see (8),

$$\mathbf{c}'(\mathbf{p})\widehat{\mathbf{p}} = (\widehat{p}_1, \widehat{p}_2, c'_{1,1}(\mathbf{p})\widehat{\mathbf{p}}, c'_{6,6}(\mathbf{p})\widehat{\mathbf{p}}, c'_{1,3}(\mathbf{p})\widehat{\mathbf{p}})^\top. \quad (23b)$$

Finally, we compose B and P to obtain

$$V := B \circ P: \mathbf{D}(\Phi) \subset L^\infty(D)^{11} \rightarrow \mathcal{L}(X), \quad V(\rho, \pi, \tau) = B(P(\rho, \pi, \tau)). \quad (24)$$

By the chain rule,

$$\begin{aligned} V'(\rho, \pi, \tau) \begin{bmatrix} \widehat{\rho} \\ \widehat{\pi} \\ \widehat{\tau} \end{bmatrix} \begin{pmatrix} \mathbf{w} \\ \psi_0 \\ \vdots \\ \psi_L \end{pmatrix} &= B'(P(\rho, \pi, \tau)) P'(\rho, \pi, \tau) \begin{bmatrix} \widehat{\rho} \\ \widehat{\pi} \\ \widehat{\tau} \end{bmatrix} \begin{pmatrix} \mathbf{w} \\ \psi_0 \\ \vdots \\ \psi_L \end{pmatrix} \\ &= \begin{pmatrix} \widehat{\rho} \mathbf{w} \\ \widetilde{\mathbf{C}}'(\mathbf{p}) \widehat{\mathbf{p}}_\pi \psi_0 \\ \widetilde{\mathbf{C}}'_u(\mathbf{p}, \tau) \begin{bmatrix} \widehat{\mathbf{p}}_\pi \\ \widehat{\tau} \end{bmatrix} \psi_1 \\ \vdots \\ \widetilde{\mathbf{C}}'_u(\mathbf{p}, \tau) \begin{bmatrix} \widehat{\mathbf{p}}_\pi \\ \widehat{\tau} \end{bmatrix} \psi_L \end{pmatrix} \end{aligned} \quad (25)$$

with the following abbreviations

$$\mathbf{p} = (M, \mu, \varepsilon, \gamma, \delta)^\top, \quad \widehat{\mathbf{p}}_\pi = (p_{\pi,1}, p_{\pi,2}, \widehat{\varepsilon}, \widehat{\gamma}, \widehat{\delta})^\top, \quad (26a)$$

and

$$p_{\pi,1} = \frac{M}{\rho} \widehat{\rho} + \frac{2M}{v_p} \widehat{v}_p - \frac{\alpha M}{1 + \alpha \tau_p} \widehat{\tau}_p, \quad p_{\pi,2} = \frac{\mu}{\rho} \widehat{\rho} + \frac{2\mu}{v_s} \widehat{v}_s - \frac{\alpha \mu}{1 + \alpha \tau_s} \widehat{\tau}_s. \quad (26b)$$

After this preparatory work, we can state the derivative of the full waveform forward operator Φ as defined in (19).

Theorem 4.2. *Under the assumptions of this section, the full waveform forward operator Φ is Fréchet differentiable at any interior point $(\rho, \pi, \tau)^\top$ of $\mathbf{D}(\Phi)$:*

For $(\widehat{\rho}, \widehat{\pi}, \widehat{\tau})^\top \in L^\infty(D)^{11}$ we have $\Phi'(\rho, \pi, \tau) \begin{bmatrix} \widehat{\rho} \\ \widehat{\pi} \\ \widehat{\tau} \end{bmatrix} = \bar{u}$ where $\bar{u} = (\bar{\mathbf{v}}, \bar{\boldsymbol{\sigma}}_0, \dots, \bar{\boldsymbol{\sigma}}_L)^\top \in \mathcal{C}([0, T], X)$ with $\bar{u}(0) = 0$ is the mild solution of

$$\rho \partial_t \bar{\mathbf{v}} = \operatorname{div} \left(\sum_{l=0}^L \bar{\boldsymbol{\sigma}}_l \right) - \widehat{\rho} \partial_t \mathbf{v}, \quad (27a)$$

$$\partial_t \bar{\boldsymbol{\sigma}}_0 = \mathbf{C}(\mathbf{p}) \varepsilon(\bar{\mathbf{v}}) + \mathbf{C}'(\mathbf{p}) \widehat{\mathbf{p}}_\pi \varepsilon(\mathbf{v}), \quad (27b)$$

$$\partial_t \bar{\boldsymbol{\sigma}}_l = \mathbf{C}_u(\mathbf{p}, \tau) \varepsilon(\bar{\mathbf{v}}) \quad (27c)$$

$$- \frac{1}{\tau_{\sigma,l}} \bar{\boldsymbol{\sigma}}_l + \mathbf{C}'_u(\mathbf{p}, \tau) \begin{bmatrix} \widehat{\mathbf{p}}_\pi \\ \widehat{\tau} \end{bmatrix} \varepsilon(\mathbf{v}), \quad l = 1, \dots, L,$$

where $\mathbf{v} \in H_0^1(D, \mathbb{R}^3)$ is the first component of the classical solution of (12), $p, \widehat{\mathbf{p}}_\pi, \mathbf{C}'$, and \mathbf{C}_u are defined in (26), (8), and (23), respectively.

For the proof of the theorem above we quote theorem 3.2 from [15] which applies to the parameter-to-solution map F with respect to (14):

$$F: \mathcal{D}(F) \subset \mathcal{L}^*(X) \rightarrow \mathcal{C}([0, T], X), \quad B \mapsto u,$$

where

$$\mathcal{D}(F) = \{B \in \mathcal{L}^*(X) : \beta_- \|x\|_X^2 \leq \langle Bx, x \rangle_X \leq \beta_+ \|x\|_X^2\}$$

for given $0 < \beta_- < \beta_+ < \infty$ and $\mathcal{L}^*(X) = \{J \in \mathcal{L}(X) : J^* = J\}$.

Theorem 4.3. Let $T > 0$, $f \in W^{1,1}([0, T], X)$, and $u_0 \in \mathcal{D}(A)$. Then, F is Fréchet differentiable at $B \in \text{int}(\mathcal{D}(F))$ with $F'(B)H = \bar{u}$, $H \in \mathcal{L}^*(X)$, where $\bar{u} \in \mathcal{C}([0, T], X)$ is the mild solution of

$$B\bar{u}'(t) + A\bar{u}(t) + BQ\bar{u}(t) = -H(u'(t) + Qu(t)), \quad t \in [0, T], \quad \bar{u}(0) = 0,$$

with $u = F(B)$ being the classical solution of (14).

Proof of theorem 4.2. By an appropriate choice of β_- and β_+ , V from (24) maps $\mathcal{D}(\Phi)$

into $\mathcal{D}(F)$. Then, $\Phi'(\rho, \pi, \tau) \begin{bmatrix} \hat{\rho} \\ \hat{\pi} \\ \hat{\tau} \end{bmatrix} = F'(V(\rho, \pi, \tau))V'(\rho, \pi, \tau) \begin{bmatrix} \hat{\rho} \\ \hat{\pi} \\ \hat{\tau} \end{bmatrix}$ and an application of theorem 4.3 with $H = V'(\rho, \pi, \tau) \begin{bmatrix} \hat{\rho} \\ \hat{\pi} \\ \hat{\tau} \end{bmatrix}$ yields

$$\begin{pmatrix} \rho \partial_t \bar{v} \\ \tilde{C}(\mathbf{p}) \partial_t \bar{\sigma}_0 \\ \tilde{C}_u(\mathbf{p}, \tau) \partial_t \bar{\sigma}_1 \\ \vdots \\ \tilde{C}_u(\mathbf{p}, \tau) \partial_t \bar{\sigma}_L \end{pmatrix} = \begin{pmatrix} \text{div} \left(\sum_{l=0}^L \bar{\sigma}_l \right) \\ \varepsilon(\bar{v}) \\ \vdots \\ \varepsilon(\bar{v}) \end{pmatrix} - \begin{pmatrix} \mathbf{0} \\ \mathbf{0} \\ \frac{1}{\tau_{\sigma,1}} \tilde{C}_u(\mathbf{p}, \tau) \bar{\sigma}_1 \\ \vdots \\ \frac{1}{\tau_{\sigma,L}} \tilde{C}_u(\mathbf{p}, \tau) \bar{\sigma}_L \end{pmatrix} \\ - V'(\rho, \pi, \tau) \begin{bmatrix} \hat{\rho} \\ \hat{\pi} \\ \hat{\tau} \end{bmatrix} \left[\begin{pmatrix} \partial_t \mathbf{v} \\ \partial_t \sigma_0 \\ \partial_t \sigma_1 \\ \vdots \\ \partial_t \sigma_L \end{pmatrix} + \begin{pmatrix} \mathbf{0} \\ \mathbf{0} \\ \frac{1}{\tau_{\sigma,1}} \sigma_1 \\ \vdots \\ \frac{1}{\tau_{\sigma,L}} \sigma_L \end{pmatrix} \right]$$

which can be casted into (27) by (25), (22) and (12b), (12c). \square

4.2.2. The adjoint. We will derive a rather explicit expression for the adjoint operator of $\Phi'(\rho, \pi, \tau)$, which requires some preparation. Again, we build upon an abstract result of [15, theorem 3.3], which we quote below for completeness.

Theorem 4.4. Under the notation and assumptions of theorem 4.3 we have

$$[F'(B)^* g] H = \int_0^T \langle H(u'(t) + Qu(t)), w(t) \rangle_X dt, \quad g \in L^2([0, T], X), \quad H \in \mathcal{L}^*(X), \quad (28)$$

where $w \in \mathcal{C}([0, T], X)$ is the mild solution of the adjoint evolution equation

$$Bw'(t) - A^*w(t) - Q^*Bw(t) = g(t), \quad t \in [0, T], \quad w(T) = 0. \quad (29)$$

To apply the abstract formulation to our concrete setting, it will be convenient to express the Fréchet derivative (8) of C as the sum

$$C'(q)h = \sum_{j=1}^5 h_j C'_j(q) \quad \text{with} \quad C'_j(q) = C'(q)e_j = T(c'(p)e_j), \quad (30)$$

where $e_j \in \mathbb{R}^5$ is the j th canonical unit vector and the meaning of $c'(p)e_j$ is given in (23b). For instance,

$$C'_1(q) = T(1, 0, 2q_3 + 1, 0, t_{1,3})^\top \quad \text{with} \quad t_{1,3} = \frac{q_1(2q_2 + 1) - q_2(q_5 + 1)}{\sqrt{(q_1 - q_2)((2q_5 + 1)q_1 - q_2)}}. \quad (31)$$

Similarly we decompose

$$C(q) \stackrel{(11)}{=} T(c_{3,3}(q), c_{5,5}(q), c_{1,1}(q), c_{6,6}(q), c_{1,3}(q))^\top = \sum_{j=1}^5 C_j(q)$$

$$\text{where } C_1(q) = T(c_{3,3}(q)e_1), \quad C_2(q) = T(c_{5,5}(q)e_2), \text{ and so on.} \quad (32)$$

For a compact notation, we finally introduce the definitions

$$D_i(q, t) := C'_i(q) \tilde{C}_u(q, t) \quad \text{and} \quad E_i(q, t) := C_i(q) \tilde{C}_u(q, t) \\ \text{for } q \in D(C), \quad t \in \mathcal{T}, \quad i = 1, \dots, 5.$$

Note that $\tilde{C}_u(q, \mathbf{1}) = \tilde{C}(q)$ for $\mathbf{1} = (1, 1, 1, 1, 1)$.

Remark 4.5. In principle, the matrix inverse $\tilde{C}_u(q, t) = C_u(q, t)^{-1}$ can be expressed explicitly in terms of the entries of $C_u(q, t)$ since only the two 3×3 diagonal blocks of $C_u(q, t)$ have to be inverted.

We are now ready to state and prove the proposed adjoint operator of Φ' .

Theorem 4.6. *Let the assumptions of theorem 4.2 hold. Then, the adjoint*

$$\Phi'(\rho, \pi, \tau)^* \in \mathcal{L}\left(L^2([0, T], X), \left(L^\infty(D)^{11}\right)'\right)$$

at $(\rho, \pi, \tau)^\top \in \mathbf{D}(\Phi)$ is given by

$$\Phi'(\rho, \pi, \tau)^* \mathbf{g} = - \begin{pmatrix} \int_0^T \left(\frac{1}{\rho} \varepsilon(\mathbf{v}) : \Sigma^\rho - \partial_t \mathbf{v} \cdot \mathbf{w} \right) dt \\ \frac{2M}{v_p} \int_0^T \varepsilon(\mathbf{v}) : \Sigma_1^\pi(\tau_p) dt \\ \frac{2\mu}{v_s} \int_0^T \varepsilon(\mathbf{v}) : \Sigma_2^\pi(\tau_s) dt \\ \int_0^T \varepsilon(\mathbf{v}) : \Sigma_3^\pi(\tau_e) dt \\ \int_0^T \varepsilon(\mathbf{v}) : \Sigma_4^\pi(\tau_g) dt \\ \int_0^T \varepsilon(\mathbf{v}) : \Sigma_5^\pi(\tau_d) dt \\ \int_0^T \varepsilon(\mathbf{v}) : \left(\Sigma_1^\tau - \frac{\alpha M}{1+\alpha\tau_p} \Sigma_1^\pi(\tau_p) \right) dt \\ \int_0^T \varepsilon(\mathbf{v}) : \left(\Sigma_2^\tau - \frac{\alpha\mu}{1+\alpha\tau_s} \Sigma_2^\pi(\tau_s) \right) dt \\ \int_0^T \varepsilon(\mathbf{v}) : \Sigma_3^\tau dt \\ \int_0^T \varepsilon(\mathbf{v}) : \Sigma_4^\tau dt \\ \int_0^T \varepsilon(\mathbf{v}) : \Sigma_5^\tau dt \end{pmatrix} \in L^1(D)^{11} \quad (33)$$

for $\mathbf{g} = (\mathbf{g}_{-1}, \mathbf{g}_0, \dots, \mathbf{g}_L)^\top \in L^2([0, T], L^2(D, \mathbb{R}^3) \times L^2(D, \mathbb{R}_{\text{sym}}^{3 \times 3})^{1+L})$, where \mathbf{v} is the first component of the solution of (12),

$$\begin{aligned} \Sigma^\rho &= (M\mathbf{D}_1(\mathbf{p}, \mathbf{1}) + \mu\mathbf{D}_2(\mathbf{p}, \mathbf{1}))\varphi_0 + (M\tau_p\mathbf{D}_1(\mathbf{p}, \tau) + \mu\tau_s\mathbf{D}_2(\mathbf{p}, \tau)) \sum_{l=1}^L \varphi_l, \\ \Sigma_i^\pi(\sigma) &= \mathbf{D}_i(\mathbf{p}, \mathbf{1})\varphi_0 + \sigma\mathbf{D}_i(\mathbf{p}, \tau) \sum_{l=1}^L \varphi_l, \quad \sigma \in \mathbb{R}, \quad \Sigma_i^\tau = \mathbf{E}_i(\mathbf{p}, \tau) \sum_{l=1}^L \varphi_l, \quad i = 1, \dots, 5, \end{aligned}$$

and $w = (\mathbf{w}, \varphi_0, \dots, \varphi_L)^\top \in \mathcal{C}([0, T], X)$ uniquely solves the adjoint state equation

$$\partial_t \mathbf{w} = \frac{1}{\rho} \operatorname{div} \left(\sum_{l=0}^L \varphi_l \right) + \frac{1}{\rho} \mathbf{g}_{-1}, \quad (34a)$$

$$\partial_t \varphi_0 = \mathbf{C}(\mathbf{p})(\varepsilon(\mathbf{w}) + \mathbf{g}_0), \quad (34b)$$

$$\partial_t \varphi_l = \mathbf{C}_u(\mathbf{p}, \tau)(\varepsilon(\mathbf{w}) + \mathbf{g}_l) + \frac{1}{t_{\sigma,l}} \varphi_l, \quad l = 1, \dots, L, \quad (34c)$$

with end condition $w(T) = \mathbf{0}$.

As a product of two $L^2(D)$ functions, each component of the right-hand side of (33) is actually a function in $L^1(D)$ which is a subspace of $L^\infty(D)'$.

Proof of theorem 4.6. Since the operators from (15) and (17) satisfy $A^* = -A$, $Q^* = Q$, and $QB = BQ$, we observe that (34) is (29) when formulated for viscoelastic VTI media. Moreover, by (28),

$$\begin{aligned}
& \left\langle \Phi'(\rho, \pi, \tau)^* \mathbf{g}, \begin{pmatrix} \hat{\rho} \\ \hat{\pi} \\ \hat{\tau} \end{pmatrix} \right\rangle_{(L^\infty(D)^{11})' \times L^\infty(D)^{11}} \\
&= \left\langle F'(V(\rho, \pi, \tau))^* \mathbf{g}, V'(\rho, \pi, \tau) \begin{pmatrix} \hat{\rho} \\ \hat{\pi} \\ \hat{\tau} \end{pmatrix} \right\rangle_{\mathcal{L}(X)' \times \mathcal{L}(X)} \\
&= \int_0^T \left\langle V'(\rho, \pi, \tau) \begin{pmatrix} \hat{\rho} \\ \hat{\pi} \\ \hat{\tau} \end{pmatrix} (u'(t) + Qu(t)), w(t) \right\rangle_X dt,
\end{aligned}$$

where $u = (\mathbf{v}, \sigma_0, \dots, \sigma_L)^\top$ is the classical solution of (12).

With (25), the integrand can be evaluated to yield

$$\begin{aligned}
\left\langle V'(\rho, \pi, \tau) \begin{pmatrix} \hat{\rho} \\ \hat{\pi} \\ \hat{\tau} \end{pmatrix} (u' + Qu), w \right\rangle_X &= \int_D \left[\hat{\rho} \partial_t \mathbf{v} \cdot \mathbf{w} + \tilde{\mathbf{C}}'(\mathbf{p}) \hat{\mathbf{p}}_\pi \partial_t \sigma_0 : \varphi_0 \right. \\
&\quad \left. + \sum_{l=1}^L \tilde{\mathbf{C}}'_u(\mathbf{p}, \tau) \left[\frac{\hat{\mathbf{p}}_\pi}{\hat{\tau}} \right] \left(\partial_t \sigma_l + \frac{\sigma_l}{t_{\sigma,l}} \right) : \varphi_l \right] dx.
\end{aligned}$$

We continue to evaluate the terms of the integrand. By (10) and the self-adjointness of the involved tensors with respect to the Frobenius inner product, we get

$$\tilde{\mathbf{C}}'(\mathbf{p}) \hat{\mathbf{p}}_\pi \partial_t \sigma_0 : \varphi_0 = -\mathbf{C}'(\mathbf{p}) \hat{\mathbf{p}}_\pi \tilde{\mathbf{C}}(\mathbf{p}) \partial_t \sigma_0 : \tilde{\mathbf{C}}(\mathbf{p}) \varphi_0 \stackrel{(12b)}{=} -\mathbf{C}'(\mathbf{p}) \hat{\mathbf{p}}_\pi \varepsilon(\mathbf{v}) : \tilde{\mathbf{C}}(\mathbf{p}) \varphi_0.$$

We apply (30) with (26) to the term on the right. Then,

$$\begin{aligned}
\tilde{\mathbf{C}}'(\mathbf{p}) \hat{\mathbf{p}}_\pi \partial_t \sigma_0 : \varphi_0 &= - \left[\left(\frac{M}{\rho} \hat{\rho} + \frac{2M}{v_p} \hat{v}_p - \frac{\alpha M}{1 + \alpha \tau_p} \hat{\tau}_p \right) \mathbf{C}'_1(\mathbf{p}) + \left(\frac{\mu}{\rho} \hat{\rho} + \frac{2\mu}{v_s} \hat{v}_s - \frac{\alpha \mu}{1 + \alpha \tau_s} \hat{\tau}_s \right) \right. \\
&\quad \left. \times \mathbf{C}'_2(\mathbf{p}) + \hat{\varepsilon} \mathbf{C}'_3(\mathbf{p}) + \hat{\gamma} \mathbf{C}'_4(\mathbf{p}) + \hat{\delta} \mathbf{C}'_5(\mathbf{p}) \right] \varepsilon(\mathbf{v}) : \tilde{\mathbf{C}}(\mathbf{p}) \varphi_0,
\end{aligned}$$

which we regroup into

$$\begin{aligned}
\tilde{\mathbf{C}}'(\mathbf{p}) \hat{\mathbf{p}}_\pi \partial_t \sigma_0 : \varphi_0 &= - \left[\hat{\rho} \left(\frac{M}{\rho} \varepsilon(\mathbf{v}) : \mathbf{D}_1(\mathbf{p}, \mathbf{1}) \varphi_0 + \frac{\mu}{\rho} \varepsilon(\mathbf{v}) : \mathbf{D}_2(\mathbf{p}, \mathbf{1}) \varphi_0 \right) \right. \\
&\quad + \hat{v}_p \left(\frac{2M}{v_p} \varepsilon(\mathbf{v}) : \mathbf{D}_1(\mathbf{p}, \mathbf{1}) \varphi_0 \right) + \hat{v}_s \left(\frac{2\mu}{v_s} \varepsilon(\mathbf{v}) : \mathbf{D}_2(\mathbf{p}, \mathbf{1}) \varphi_0 \right) \\
&\quad + \hat{\varepsilon}(\varepsilon(\mathbf{v}) : \mathbf{D}_3(\mathbf{p}, \mathbf{1}) \varphi_0) + \hat{\gamma}(\varepsilon(\mathbf{v}) : \mathbf{D}_4(\mathbf{p}, \mathbf{1}) \varphi_0) + \hat{\delta}(\varepsilon(\mathbf{v}) : \mathbf{D}_5(\mathbf{p}, \mathbf{1}) \varphi_0) \\
&\quad \left. - \hat{\tau}_p \left(\frac{\alpha M}{1 + \alpha \tau_p} \varepsilon(\mathbf{v}) : \mathbf{D}_1(\mathbf{p}, \mathbf{1}) \varphi_0 \right) - \hat{\tau}_s \left(\frac{\alpha \mu}{1 + \alpha \tau_s} \varepsilon(\mathbf{v}) : \mathbf{D}_2(\mathbf{p}, \mathbf{1}) \varphi_0 \right) \right].
\end{aligned}$$

Now we consider

$$\begin{aligned} \tilde{C}'_u(\mathbf{p}, \tau) \left[\frac{\hat{\mathbf{p}}_\pi}{\hat{\tau}} \right] \left(\partial_t \sigma_l + \frac{\sigma_l}{t_{\sigma,l}} \right) : \varphi_l &= -C'_u(\mathbf{p}, \tau) \left[\frac{\hat{\mathbf{p}}_\pi}{\hat{\tau}} \right] \tilde{C}_u(\mathbf{p}, \tau) \left(\partial_t \sigma_l + \frac{\sigma_l}{t_{\sigma,l}} \right) : \tilde{C}_u(\mathbf{p}, \tau) \varphi_l \\ &\stackrel{(23), (12c)}{=} -C_u(\mathbf{p}, \hat{\tau}) \varepsilon(\mathbf{v}) : \tilde{C}_u(\mathbf{p}, \tau) \varphi_l - \mathbf{T}(\tau \odot \mathbf{c}'(\mathbf{p}) \hat{\mathbf{p}}_\pi) \varepsilon(\mathbf{v}) : \tilde{C}_u(\mathbf{p}, \tau) \varphi_l. \end{aligned}$$

We can handle $\mathbf{T}(\tau \odot \mathbf{c}'(\mathbf{p}) \hat{\mathbf{p}}_\pi) \varepsilon(\mathbf{v}) : \tilde{C}_u(\mathbf{p}, \tau) \varphi_l$ by analogy with $C'(\mathbf{p}) \hat{\mathbf{p}}_\pi \varepsilon(\mathbf{v}) : \tilde{C}(\mathbf{p}) \varphi_0$ from above. Thus,

$$\begin{aligned} \mathbf{T}(\tau \odot \mathbf{c}'(\mathbf{p}) \hat{\mathbf{p}}_\pi) \varepsilon(\mathbf{v}) : \tilde{C}_u(\mathbf{p}, \tau) \varphi_l &= \hat{\rho} \left(\frac{M\tau_p}{\rho} \varepsilon(\mathbf{v}) : \mathbf{D}_1(\mathbf{p}, \tau) \varphi_l + \frac{\mu\tau_s}{\rho} \varepsilon(\mathbf{v}) : \mathbf{D}_2(\mathbf{p}, \tau) \varphi_l \right) \\ &\quad + \hat{v}_p \left(\frac{2M\tau_p}{v_p} \varepsilon(\mathbf{v}) : \mathbf{D}_1(\mathbf{p}, \tau) \varphi_l \right) + \hat{v}_s \left(\frac{2\mu\tau_s}{v_s} \varepsilon(\mathbf{v}) : \mathbf{D}_2(\mathbf{p}, \tau) \varphi_l \right) \\ &\quad + \hat{\varepsilon}(\tau_e \varepsilon(\mathbf{v}) : \mathbf{D}_3(\mathbf{p}, \tau) \varphi_l) + \hat{\gamma}(\tau_g \varepsilon(\mathbf{v}) : \mathbf{D}_4(\mathbf{p}, \tau) \varphi_l) + \hat{\delta}(\tau_d \varepsilon(\mathbf{v}) : \mathbf{D}_5(\mathbf{p}, \tau) \varphi_l) \\ &\quad - \hat{\tau}_p \left(\frac{\alpha M\tau_p}{1 + \alpha\tau_p} \varepsilon(\mathbf{v}) : \mathbf{D}_1(\mathbf{p}, \tau) \varphi_l \right) - \hat{\tau}_s \left(\frac{\alpha\mu\tau_s}{1 + \alpha\tau_s} \varepsilon(\mathbf{v}) : \mathbf{D}_2(\mathbf{p}, \tau) \varphi_l \right). \end{aligned}$$

Using (11) and (32) we get

$$\begin{aligned} C_u(\mathbf{p}, \hat{\tau}) \varepsilon(\mathbf{v}) : \tilde{C}_u(\mathbf{p}, \tau) \varphi_l &= \hat{\tau}_p (\varepsilon(\mathbf{v}) : \mathbf{E}_1(\mathbf{p}, \tau) \varphi_l) + \hat{\tau}_s (\varepsilon(\mathbf{v}) : \mathbf{E}_2(\mathbf{p}, \tau) \varphi_l) \\ &\quad + \hat{\tau}_e (\varepsilon(\mathbf{v}) : \mathbf{E}_3(\mathbf{p}, \tau) \varphi_l) + \hat{\tau}_g (\varepsilon(\mathbf{v}) : \mathbf{E}_4(\mathbf{p}, \tau) \varphi_l) \\ &\quad + \hat{\tau}_d (\varepsilon(\mathbf{v}) : \mathbf{E}_5(\mathbf{p}, \tau) \varphi_l). \end{aligned}$$

By these evaluations we find that

$$\begin{aligned} &\left\langle V'(\rho, \pi, \tau) \left(\frac{\hat{\rho}}{\hat{\pi}} \right) (u' + Qu), w \right\rangle_X \\ &= \int_D \left[\hat{\rho} \left(\partial_t \mathbf{v} \cdot \mathbf{w} - \frac{1}{\rho} \varepsilon(\mathbf{v}) : \Sigma^\rho \right) - \hat{v}_p \left(\frac{2M}{v_p} \varepsilon(\mathbf{v}) : \Sigma_1^\pi(\tau_p) \right) - \hat{v}_s \left(\frac{2\mu}{v_s} \varepsilon(\mathbf{v}) : \Sigma_2^\pi(\tau_s) \right) \right. \\ &\quad - \hat{\varepsilon}(\varepsilon(\mathbf{v}) : \Sigma_3^\pi(\tau_e)) - \hat{\gamma}(\varepsilon(\mathbf{v}) : \Sigma_4^\pi(\tau_g)) - \hat{\delta}(\varepsilon(\mathbf{v}) : \Sigma_5^\pi(\tau_d)) \\ &\quad + \hat{\tau}_p \left(\varepsilon(\mathbf{v}) : \left(\Sigma_1^\tau - \frac{\alpha M}{1 + \alpha\tau_p} \Sigma_1^\pi(\tau_p) \right) \right) + \hat{\tau}_s \left(\varepsilon(\mathbf{v}) : \left(\Sigma_2^\tau - \frac{\alpha\mu}{1 + \alpha\tau_s} \Sigma_2^\pi(\tau_s) \right) \right) \\ &\quad \left. - \hat{\tau}_e (\varepsilon(\mathbf{v}) : \Sigma_3^\tau) - \hat{\tau}_g (\varepsilon(\mathbf{v}) : \Sigma_4^\tau) - \hat{\tau}_d (\varepsilon(\mathbf{v}) : \Sigma_5^\tau) \right] dx. \end{aligned}$$

Integrating both sides in time from 0 to T and changing the order of integration leads to the stated expression for $\Phi'(\rho, \pi, \tau) * \mathbf{g}$. \square

Remark 4.7. We point out that the tensors $C_i(\mathbf{p})$ and $C'_i(\mathbf{p})$ being part of $\mathbf{E}_i(\mathbf{p}, \tau)$ and $\mathbf{D}_i(\mathbf{p}, \tau)$, respectively, can be further decomposed into linear combinations of the 5 basis tensors $\mathbf{T}(\mathbf{e}_i)$, $i = 1, \dots, 5$. Then, only the scalars in front of the basis tensors depend on the material parameters. For instance,

$$C_4(\mathbf{p}) \stackrel{(32)}{=} c_{6,6}(\mathbf{p}) \mathbf{T}(\mathbf{e}_4) = (2\gamma + 1) \mu \mathbf{T}(\mathbf{e}_4)$$

and

$$\mathbf{C}'_1(\mathbf{p}) \stackrel{(31)}{=} \mathbf{T}(\mathbf{e}_1) + (2\varepsilon + 1) \mathbf{T}(\mathbf{e}_3) + \frac{M(2\mu + 1) - \mu(\delta + 1)}{\sqrt{(M - \mu)((2\delta + 1)M - \mu)}} \mathbf{T}(\mathbf{e}_5).$$

For a compact and clearer presentation of the previous theorem, we have dispensed with this granular decomposition.

5. Concluding remarks

5.1. Other anisotropic media

The techniques to obtain the Fréchet derivative and its adjoint for the viscoelastic FWI forward operator, which we have demonstrated in the previous sections, transfer to the corresponding operators for other anisotropic media, such as tilted transverse isotropic (TTI) and monoclinic media, see, e.g. [5]. In a TTI medium, for example, the vertical rotational symmetry axis of the VTI medium is tilted by the angles θ_v and θ_h in the vertical x_1 - x_3 -plane and the horizontal x_1 - x_2 -plane, respectively. In such a way, TTI media model the tilt of strata due to tectonic movement. The corresponding stiffness tensor can be obtained from the VTI tensor by a local rotation $O(\theta_v, \theta_h)$ (Bond transformation, see, e.g. [5]), that is, the tilt angles are spatially dependent functions and

$$\mathbf{C}_u^{\text{TTI}}(\mathbf{p}, \boldsymbol{\tau}, \theta_v, \theta_h) = O(\theta_v, \theta_h) \mathbf{C}_u(\mathbf{p}, \boldsymbol{\tau}) O(\theta_v, \theta_h)^\top.$$

Hence, three-dimensional FWI in attenuating TTI media inverts for 13 parameter functions. See [18] for a two-dimensional example, however, without attenuation.

5.2. The two-dimensional case

Our results include the two-dimensional situation as well. We only need to set the partial derivatives of the stress components with respect to x_2 in (12) to zero. Then the wave equation decomposes into two independent systems describing the P/SV case and the SH case. For instance, the stiffness tensor for the P/SV case is the 3×3 matrix

$$\mathbf{C} = \begin{pmatrix} c_{1,1} & c_{1,3} & 0 \\ c_{1,3} & c_{3,3} & 0 \\ 0 & 0 & c_{5,5} \end{pmatrix},$$

whose entries are still given by (4). Horizontally polarized S-waves occur only in the SH case, where the stiffness tensor is the 2×2 diagonal matrix with entries $c_{6,6}$ and $c_{5,5}$.

Data availability statement

The data that support the findings of this study are openly available at the following URL/DOI: <https://gitlab.kit.edu/kigpi/ag/software/sofi2d>.

Acknowledgment

The author thanks Thomas Bohlen from the Geophysical Institute at KIT for sharing his expertise.

ORCID iD

Andreas Rieder  <https://orcid.org/0000-0002-3192-2847>

References

- [1] Blanch J O, Robertsson J O A and Symes W W 1995 Modeling of a constant Q: methodology and algorithm for an efficient and optimally inexpensive viscoelastic technique *Geophysics* **60** 176–84
- [2] Bohlen T 1998 Viskoelastische FD-Modellierung seismischer Wellen zur Interpretation gemessener Seismogramme *PhD Thesis* Christian-Albrechts-Universität zu Kiel
- [3] Bohlen T 2002 Parallel 3-D viscoelastic finite difference seismic modelling *Comput. Geosci.* **28** 887–99
- [4] Bohlen T, Fernandez M R, Ernesti J, Rheinbay C, Rieder A and Wieners C 2021 Visco-acoustic full waveform inversion: from a DG forward solver to a Newton-CG inverse solver *Comput. Math. Appl.* **100** 126–40
- [5] Carcione J 2015 *Wave Fields in Real Media: Wave Propagation in Anisotropic, Anelastic, Porous and Electromagnetic Media* 3rd edn (Elsevier Science)
- [6] Dörfler W, Hochbruck M, Köhler J, Rieder A, Schnaubelt R and Wieners C 2023 *Wave Phenomena—Mathematical Analysis and Numerical Approximation (Oberwolfach Seminars vol 49)* (Birkhäuser/Springer)
- [7] Duvaut G and Lions J-L 1976 *Inequalities in Mechanics and Physics (Grundlehren der Mathematischen Wissenschaften vol 219)* (Springer) Translated from the French by C. W. John
- [8] Epanomeritakis I, Akcelik V, Ghattas O and Bielak J 2008 A Newton-CG method for large-scale three-dimensional elastic full-waveform seismic inversion *Inverse Problems* **24** 034015
- [9] Fichtner A 2011 *Full Seismic Waveform Modelling and Inversion (Advances in Geophysical and Environmental Mechanics and Mathematics)* (Springer)
- [10] Gercek H 2007 Poisson's ratio values for rocks *Int. J. Rock Mech. Mining Sci.* **44** 1–13
- [11] Gould P L and Feng Y 2018 *Introduction to Linear Elasticity* 4th edn (Springer)
- [12] Ito K and Kappel F 2002 *Evolution Equations and Approximations (Series on Advances in Mathematics for Applied Sciences vol 61)* (World Scientific Publishing Co., Inc.)
- [13] Jones L E A and Wang H F 1981 Ultrasonic velocities in Cretaceous shales from the Williston basin *Geophysics* **46** 288–97
- [14] Kirsch A and Rieder A 2016 Inverse problems for abstract evolution equations with applications in electrodynamics and elasticity *Inverse Problems* **32** 085001
- [15] Kirsch A and Rieder A 2019 Inverse problems for abstract evolution equations II: higher order differentiability for viscoelasticity *SIAM J. Appl. Math.* **79** 2639–62
Kirsch A and Rieder A 2022 Corrigendum to 'Inverse Problems for abstract evolution equations II: higher order differentiability for viscoelasticity' (arXiv:2203.01309)
- [16] Krampe V, Pan Y and Bohlen T 2019 Two-dimensional elastic full-waveform inversion of Love waves in shallow vertically transversely isotropic media: synthetic reconstruction tests *Near Surface Geophys.* **17** 449–61
- [17] Métivier L, Brossier R, Virieux J and Operto S 2013 Full waveform inversion and the truncated Newton method *SIAM J. Sci. Comput.* **35** B401–37
- [18] Oh J-W, Shin Y, Alkhalifah T and Min D-J 2020 Multistage elastic full-waveform inversion for tilted transverse isotropic media *Geophys. J. Int.* **223** 57–76
- [19] Robertsson J O, Blanch J O and Symes W W 1994 Viscoelastic finite-difference modeling *Geophysics* **59** 1444–56
- [20] Sortan S A 2022 Effects of seismic anisotropy and attenuation on first-arrival waveforms recorded at the Asse II nuclear repository *Master's Thesis* Karlsruhe Institute of Technology, Karlsruhe (<https://doi.org/10.5445/IR/1000151635>)

- [21] Tarantola A 1988 Theoretical background for the inversion of seismic waveforms including elasticity and attenuation *Pure Appl. Geophys.* **128** 365–99
- [22] Thomsen L 1986 Weak elastic anisotropy *Geophysics* **51** 1954–66
- [23] Tsvankin I 2001 *Signatures and Analysis of Reflection Data in Anisotropic Media (Handbook of Geophysical Exploration: Seismic Exploration vol 29)* (Pergamon)
- [24] Yang P, Brossier R, Métivier L, Virieux J and Zhou W 2018 A time-domain preconditioned truncated Newton approach to visco-acoustic multiparameter full waveform inversion *SIAM J. Sci. Comput.* **40** B1101–30
- [25] Zeltmann U 2018 The viscoelastic seismic model: existence, uniqueness and differentiability with respect to parameters *PhD Thesis* Karlsruhe Institute of Technology (<https://doi.org/10.5445/IR/1000093989>)